THE $\Delta I = 1/2$ RULE FOR $K \to \pi\pi$ DECAYS*

BY J. O. EEG

Institute of Physics, University of Oslo**

(Received October 7, 1986)

Attempts to explain the $\Delta I = 1/2$ rule in $K \to \pi\pi$ decays are discussed. The standard effective Hamiltonian approach to non-leptonic decays is shortly reviewed. Recent long distance approaches, some of which give encouraging results, are described. It is concluded that long distance approaches to the penguin diagram improves the understanding of the $\Delta I = 1/2$ rule.

PACS numbers: 13.20.Eb

1. Introduction

In spite of the general success of the standard model, a satisfactory explanation of the well established $\Delta I = 1/2$ rule for $K \to \pi\pi$ decays still seems to be lacking. Experimentally, this rule can be expressed as

$$\frac{\Gamma(K_S^0 \to \pi^+\pi^-)}{\Gamma(K^\pm \to \pi^\pm\pi^0)} \simeq 450. \tag{1}$$

The basic non-leptonic strangeness changing interaction, which is diagrammatically shown in Fig. 1, may at the free quark level be written as a product of two left-handed currents:

$$H_W^{(0)} \sim G_F \sin\theta_C \cos\theta_C j^W(su)_\mu j^W(ud)^\mu, \tag{2a}$$

where G_F is Fermi's coupling constant and θ_C the Cabibbo angle.

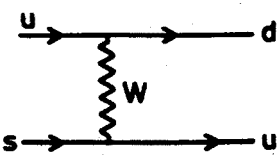

Fig. 1. The basic non-leptonic interaction at quark level

* Based on lectures given at the XXVI Cracow School of Theoretical Physics, Zakopane, Poland, June 1–13, 1986.

** Address: Department of Physics, University of Oslo, P. O. Box 1048, Blindern 0316, Oslo 3, Norway.

$$j^{W}(su)_{\mu} = \bar{u}_{L}\gamma_{\mu}s_{L} = \bar{u}\gamma_{\mu}Ls; \quad [\psi_{L} \equiv L\psi, L \equiv \tfrac{1}{2}(1-\gamma_{5})] \tag{2b}$$

is the left-handed quark current. During the last decade, non-leptonic decays have mostly been analysed [1–3] in terms of an effective weak Hamiltonian consisting of local four quark operators multiplied with coefficients determined by the renormalization group equations (RGE). Eq. (2) is the "bare" (i.e. free quark) version of this Hamiltonian H_{W}. Theoretically, the $\Delta I = 1/2$ rule states that the matrix elements of $H_{W}(\Delta I = 1/2)$ dominates over $H_{W}(\Delta I = 3/2)$. However, the bare basic interaction (2) involves $\Delta I = 1/2$ and $\Delta I = 3/2$ parts of comparable magnitude. Typical quark diagrams for $K \to \pi\pi$ are given in Fig. 2.

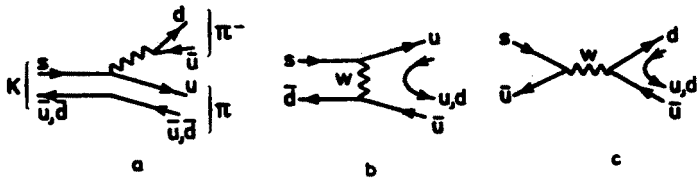

Fig. 2. Typical quark diagrams for $K \to \pi\pi$ (gluon interactions are not shown): a) The quark decay mechanism thought to be dominant. b) The exchange mechanism. c) The annihilation mechanism. b) and c) are related through a Fierz transformation)

It is often convenient to use "pion reduction" (current algebra and soft pion limit) to relate the physical $K \to \pi\pi$ amplitudes and the off-shell $K \to \pi$ transition. These relations can be written in terms of two dimensionless quantities $D(\Delta I = 1/2)$ and $D(\Delta I = 3/2)$ parametrizing $\Delta I = 1/2$ and $\Delta I = 3/2$ amplitudes respectively:

$$A(K_{S}^{0} \to \pi^{+}\pi^{-})_{\Delta I=1/2} = \frac{i}{\sqrt{2}}\hat{G}f_{\pi}(m_{K}^{2}-m_{\pi}^{2})D(\Delta I = 1/2), \tag{3a}$$

$$A(K^{-} \to \pi^{-}\pi^{0})_{\Delta I=3/2} = \tfrac{3}{2}\frac{i}{\sqrt{2}}\hat{G}f_{\pi}(m_{K}^{2}-m_{\pi}^{2})D(\Delta I = 3/2), \tag{3b}$$

$$A(K^{-} \to \pi^{-})_{\Delta I=1/2,3/2} = -\tfrac{1}{2}\hat{G}f_{\pi}f_{K}p_{K}\cdot p_{\pi}D(\Delta I = 1/2, 3/2), \tag{3c}$$

where $\hat{G} \equiv \sqrt{2}\,G_{F}\sin\theta_{C}\cos\theta_{C}$. It should be emphasized [4] that the $K \to \pi$ transition must be proportional to the product of the (off-shell) K and π momenta. This property follows from chiral Lagrangians [4, 5] and within the so-called vacuum insertion approximation, where

$$j^{W}(su)^{\mu} \sim f_{K}p_{K}^{\mu}, \quad j^{W}(ud)^{\mu} \sim f_{\pi}p_{\pi}^{\mu}, \tag{4}$$

for the $K \to \pi$ transition. Our task is then to calculate the ratio

$$r \equiv \frac{D(\Delta I = 1/2)}{D(\Delta I = 3/2)}. \tag{5}$$

From the bare interaction (2) one obtains $r = 5/4$ in the vacuum insertion approximation, while the experimental value obtained from (1) is [4]

$$|r|_{\text{exp}} \simeq 32. \tag{6}$$

This big number has been a great challenge to theorists. In 1974, perturbative QCD corrections (see Fig. 3) to the effective weak $\Delta S = 1$ Hamiltonian was performed. The calculations gave qualitatively an enhancement of $\Delta I = 1/2$ amplitudes, but the result was numerically only a partial success [1]. Later, Shifman, Vainshtein and Zakharov (SVZ) [2] proposed that the so-called penguin diagram (see Fig. 4) could explain the $\Delta I = 1/2$

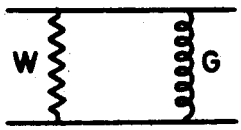

Fig. 3. QCD corrections of order α_s to the "bare" interaction in Fig. 1

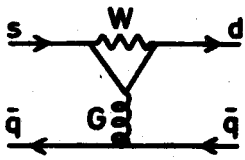

Fig. 4. The "penguin" diagram

rule. This diagram corresponds to a pure $\Delta I = 1/2$ transition and introduces operators of "left-right" type (i.e. involving a product of a left-handed and a right-handed current) in addition to the pure "left-left" operators occurring in the effective Hamiltonian of Ref. [1]. It was argued [2] that even if the Wilson coefficients of the new left-right operators are small compared to those of the left-left operators, their matrix elements for $K \to \pi$ might be big enough to give an explanation of the $\Delta I = 1/2$ rule. This has recently been questioned by several authors. Moreover, to obtain a short distance behaviour of the penguin diagram, the charmed quark mass is formally considered to be big compared to the typical hadronic mass scale, which is also questionable. Certainly the penguin diagram generates a pure $\Delta I = 1/2$ interaction, but the question is how to handle it and how important it is.

In general, there seems to be a growing feeling among physicists working in the field that the long distance aspects of $K \to \pi\pi$ decays are important [6–10]. To be more specific, recent lattice calculations [9] considering so-called "eight graphs" (basically corresponding to left-left interactions of Ref. [1]) and "eye-graphs" (basically corresponding to the penguin diagram) show a dominance of "eye-graphs", which indicates an explanation of the $\Delta I = 1/2$ rule. On the other hand, a recent analysis [10] in terms of QCD sum rules and chiral Lagrangians fails to explain the $\Delta I = 1/2$ rule. In Section 3 some recent long distance approaches are shortly reviewed. In some recent papers I have proposed that the penguin diagram should (mainly) be treated as a long distance effect [6–8]. That is, the dominating

contribution to the penguin diagram is due to low loop momenta where confinement effects are importan.. This low momentum approach to the penguin diagram is presented in Section 4. Discussion and conclusion are given in Section 5.

2. *The effective Hamiltonian approach*

a) Perturbative QCD corrections

Formally, non-leptonic $\Delta S = 1$ interactions can be described by the time ordered product of two weak current operators J_μ^W:

$$H_W(x) \sim \int d^4y T\{J_\mu^W(x) J_\nu^W(y)\} D_W^{\mu\nu}(x-y), \tag{7}$$

where D_W is the W-boson propagator. In the limit where the W-boson is considered as heavy, the weak Hamiltonian (density) H_W can be written as a short distance expansion [1–3]

$$H_W = \hat{G} \sum_i C_i(\mu) Q_i(\mu), \tag{8}$$

where $\hat{G}$ is given below Eq. (3) (we restrict ourselves to four flavours because we do not consider CP-violating effects). The Q_i's are four quark operators and the corresponding coefficients C_i are determined by RGE. These depend on the renormalization point μ. The matrix elements of H_W between hadronic states — i.e. the physical amplitudes — must of course be independent of μ. The first calculation of the weak Hamiltonian of the form (8) — taking into account QCD corrections to first order in the strong fine structure constant α_S — was performed by Gaillard and Lee [1a] and by Altarelli and Maiani [1b]. Their H_W involved two quark operators $Q_\pm$:

$$H_W = \hat{G}[C_+ Q_+ + C_- Q_-], \tag{9a}$$

$$Q_\pm = Q_A \pm Q_B, \tag{9b}$$

$$Q_A = \bar{d}\gamma^\mu L u \bar{u}\gamma_\mu L s - (u \to c), \tag{9c}$$

$$Q_B = \bar{u}\gamma^\mu L u \bar{d}\gamma_\mu L s - (u \to c). \tag{9d}$$

The operator Q_A corresponds to the free quark diagram in Fig. 1 (see also Fig. 5a), while Q_B is induced by the QCD diagram in Fig. 3 (see also Fig. 5b). The explanation

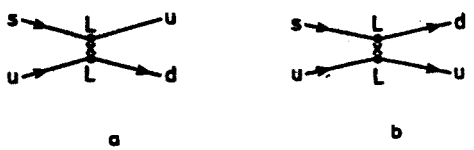

Fig. 5. Diagrammatic representations of the operators Q_A and Q_B (for W considered as "heavy")

for this is easy when remembering that exchange of a gluon involves the colour matrix product

$$t^a_{ij}t^a_{kl} = \tfrac{1}{2}\left[\delta_{il}\delta_{jk} - \frac{1}{N_c}\,\delta_{ij}\delta_{kl}\right], \tag{10}$$

where i, j, k, l are colour indices for the quarks, and $N_c = 3$ the number of colours. Using in addition the Fierz transformation

$$\bar{\psi}_A\gamma_\mu L\psi_B\,\bar{\psi}_C\gamma^\mu L\psi_D = \bar{\psi}_A\gamma_\mu L\psi_D\,\bar{\psi}_C\gamma^\mu L\psi_B, \tag{11}$$

it is easily seen that the first term on the right hand side of (10) gives the operator Q_B. From a RGE-analysis one obtains the coefficients [1]

$$C_\pm(\mu) = \left(\frac{\alpha_S(\mu^2)}{\alpha_S(M_W^2)}\right)^{\gamma_\pm} = \left[1 + b\,\frac{\alpha_S(\mu^2)}{4\pi}\ln\left(\frac{M_W^2}{\mu^2}\right)\right]^{\gamma_\pm}, \tag{12a}$$

where $b = 11 - 2N_F/3$ (N_F being the number of flavours) and the quantities $\gamma_\pm$ are determined by the anomalous dimensions of the operators $Q_\pm$. For $\mu \lesssim 1$ GeV and $\alpha_S(\mu^2) \simeq 1$, one obtains numerically

$$C_+ \simeq 0.7, \quad C_- \simeq 2.5, \tag{12b}$$

while the bare values are $C_\pm^{(0)} = 1$. Using the effective Hamiltonian in (9), one obtains the $K \to \pi$ transition amplitudes (see Eq. (3))

$$D^{(LL)}(\Delta I = 1/2) = \tfrac{2}{3}\,[C_-Z_- + \tfrac{2}{3}\,C_+Z_+], \tag{13a}$$

$$D^{(LL)}(\Delta I = 3/2) = \tfrac{8}{9}\,C_+Z_+, \tag{13b}$$

where $Z_\pm$ are factors to correct for the vacuum insertion approximation described below Eq. (3). (The superscript LL indicates that the left-left structure Hamiltonian of Ref. [1] is used.) It is shown [11] that $Z_\pm < 1$. More specific, $Z_\pm$ are probably bigger than 1/2. Experimentally, to fit the $\Delta I = 3/2$ amplitude from (13b), $Z_+ \simeq 0.6$ [4]. This is also in agreement with a recent QCD sum rule calculation of the $\Delta I = 3/2$ amplitude [12]. For the ratio defined in (4) one obtains from (13)

$$r = \tfrac{1}{2}\left[1 + \frac{3C_-Z_-}{2C_+Z_+}\right] \simeq 3 \text{ to } 4. \tag{14}$$

Qualitatively, this ratio goes in the right direction compared to the bare result 5/4, but is numerically still far below the experimental value in (6).

b) The penguin diagram

It was noted in 1975 by Shifman, Vainstein and Zakharov (SVZ) [2] that the so-called penguin diagram (see Fig. 4) was of the same order of magnitude as the QCD corrected

diagram (Fig. 3) of Ref. [1] — and that this diagram induced a pure $\Delta I = 1/2$ interaction. Considering W as heavy, and using a Fierz transformation, the penguin diagram is drawn as in Fig. 6. Due to the GIM- mechanism [13], the high loop momenta in the u- and c-quark loops will approximately cancel, and the result is in the leading logarithmic approximation (for $m_c^2 \gg |k^2| \gg m_u^2$) proportional to

$$\frac{1}{k^2} \cdot \left[k^2 \ln\left(\frac{m_c^2}{|k^2|}\right)\right], \tag{15}$$

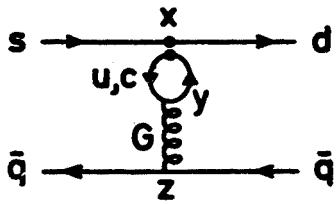

Fig. 6. Fierz-transformed version of the penguin diagram (for W considered as "heavy")

where k is the gluon momentum. The expression in brackets is the result of the loop integration. It should be emphasized that the factor k^2 from the loop calculation is cancelled by the propagator factor $1/k^2$ and thus the penguin diagram induces (when only dominant terms are kept) a local interaction

$$H_W^{(LR)} = \hat{G} C_{LR} Q_P, \tag{16a}$$

where

$$Q_P = \bar{d}\gamma_\mu L s \sum_{q=u,d,s} \bar{q}\gamma^\mu R q, \tag{16b}$$

$$C_{LR} \sim \frac{\alpha_s(\mu^2)}{4\pi} \ln\left(\frac{m_c^2}{\mu^2}\right) \sim 10^{-1}. \tag{16c}$$

μ is the renormalization point for quark and gluon momenta, i.e. $|k^2| \sim \mu^2$. The smallness of C_{LR} reflects the GIM-mechanism [13]. (Strictly speaking, there are two penguin operators. But using colour symmetry, their effect can be described in terms of one operator and one coefficient.) One should note that the vector quark current at the lower vertex in the penguin diagram can be divided in a left- and a right-handed part, while the weak interaction is purely left-handed. Thus the penguin diagram can be divided in a left-left (LL) and a left-right (LR) part. The LL part is small compared to the LL interaction in (9). The point of SVZ was that Q_P is of left-right type. And because of this new chiral structure, $H_W^{(LR)}$ might have bigger matrix elements than the operators $Q_\pm$ of (9):

$$A^{(LR)}(K^- \to \pi^-) \sim \hat{G} f_K f_\pi \frac{m_K^2 m_\pi^2 C_{LR}}{[m_u + m_d]\,[m_s + m_u]}. \tag{17}$$

This is due to the *current* quark masses in the denominator obtained by combining a Fierz transformation with PCAC:

$$\bar{\psi}_A \gamma_\mu L \psi_B \bar{\psi}_C \gamma^\mu R \psi_D = -2 \psi_A R \psi_D \bar{\psi}_C L \psi_B, \tag{18a}$$

$$\partial_\mu j^\mu_A \sim [m_u + m_{s,d}] \bar{\psi}_u \gamma_5 \psi_{s,d} \sim (m_{K,\pi})^2 \phi_{K,\pi}, \tag{18b}$$

where ψ is a quark field and ϕ a meson field.

Depending on the values of μ it has been argued that the expression (17) has some chance to explain the $\Delta I = 1/2$ rule. However, as pointed out by Dupont and Pham [4], the amplitude (17) does not satisfy the chiral constraint (3c). The solution to this problem was found by Donoghue and Gavela et al. [14]. By taking into account additional tadpole diagrams (see Fig. 8b) corresponding to so-called anomalous commutator terms [3, 14, 15]

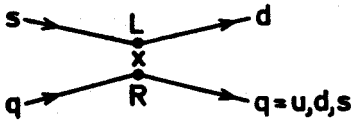

Fig. 7. Diagrammatic representation of the penguin diagram induced left-right operator Q_P

Fig. 8. Quark diagrams for $K \to \pi$ due to Q_P

it was shown that the right hand side of (17) has to be multiplied by an extra factor $p_K \cdot p_\pi / \Lambda^2$, where $\Lambda \sim 1$ GeV. Thus the chiral constraint (3c) is restored, but $A^{(LR)}$ is now suppressed by a mass factor Λ^{-2}, and according to the corrected version [14] of (17), the penguin diagram seems to be unable to explain the $\Delta I = 1/2$ rule [14a, 16]. It should however be emphasized that it is the standard short distance approach of the penguin diagram [2] combined with the use of (18) which ceases to explain the $\Delta I = 1/2$ rule. The value of C_{LR} is somewhat uncertain (for a further discussion, see subsection c) below). In a rather phenomenological approach one could therefore take C_{LR} as a free parameter [2b, 3, 17]. However, fitting C_{LR} to explain the $\Delta I = 1/2$ rule, one may come in conflict with the upper limit on the process $\Omega \to \gamma \Xi$ [18]. This process depends on the penguin diagram (where a photon can be emitted from one of the external legs of Fig. 4) but not on the ordinary left-left interactions (i.e. the diagrams in Fig. 1 and 3).

c) μ-(in-)dependence

Weak non-leptonic processes are given by matrix elements of the weak Hamiltonian H_W between hadronic states $|h\rangle$ and $|h'\rangle$:

$$\langle h' | H_W | h \rangle = \hat{G} \sum_i C_i(\mu) \langle Q_i \rangle, \tag{19a}$$

$$\langle Q_i \rangle \equiv \langle h' | Q_i(\mu) | h \rangle. \tag{19b}$$

Our problem is now that the calculation of the matrix elements $\langle Q_i \rangle$ is a non-perturbative question. Even if lattice calculations seem to be promising [9], one should at the moment still consider various model dependent calculations of the matrix elements. Such calculations have extensively been given in the literature, for instance in terms of the vacuum insertion approximation [2, 3, 17], the bag model [3, 17, 19], the harmonic oscillator model [17, 20], and the Skyrme model [21]. Bounds on matrix elements from QCD sum rules have been given in Refs [11] and [15]. Performing model dependent calculations of the matrix elements we encounter a problem: The renormalization scale μ is not a parameter in the model dependent calculations. Thus the μ-dependence of the $\langle Q_i \rangle$'s is lost, and performing practical calculations, one has to argue for a "reasonable" choice of the value of μ to be used in the coefficients C_i. One may of course argue that μ is of the same order of magnitude as some typical mass parameter in the model. However, the model result of $\langle Q_i \rangle$ need not coincide with the true value for any μ. This kind of arbitrariness is of course unsatisfactory. These problems have been discussed by Buras and Słomiński [22].

The ambiguity due to the "choice of μ" is numerically not a problem for the leading log corrections $\sim \ln [M_W^2/\mu^2]$ of Ref. [1]. However, the leading log expression (16c) for C_{LR} is for $m_c \simeq 1.4$ GeV and $\mu \sim 1$ GeV very sensitive for the specific value used for μ. Moreover, for such values of m_c and μ, $\ln(m_c^2/\mu^2)$ is hardly any leading log. It should be noted, that the expression for C_{LR} in (16c) is only valid in the leading log approximation. Using the exact expression for the penguin loop calculation, the (naive) value obtained for C_{LR} is nonzero for $\mu = m_c$ [18, 23]. It should be emphasized that when/if a model dependent calculation scheme for hadronic matrix elements is chosen, the choice of μ must be consistent with that model. (That is, if it is reasonable that a model calculation of a matrix element corresponds to $\mu \simeq \Lambda_{QCD}$, say, it is inconsistent to use $\mu = 1$ GeV in the C_i's.) This means that for the diagrams in Figs 3 and 4, contributions from low loop momenta $p < \mu$ must be regarded as part of the wave function and/or the quark propagators and vertices must be modified due to confinement for loop momenta $p < \mu$. Only in this way we can count all contributions and avoid double counting [8]. Such low momentum loop contributions will be considered in Section 4.

3. *Recent approaches to* $K \to \pi\pi$

a) Lattice calculations

As emphasized previously, the calculation of the matrix elements of the weak operators is a non-perturbative question, and one may hope to calculate these by means of lattice gauge theory [24]. Recent lattice calculations of weak operators by Bernard et al. [9] seem to be promising. These authors use pion reduction and consider the matrix element of the operators $Q_\pm$ between π and K states. (There is at present a controversy [25, 26] whether also the $K \to$ vacuum transition amplitude plays a role.) Then these states are replaced by their quark field content (i.e. $|\pi^-\rangle = \bar{u}\gamma_5 d|0\rangle$), and the authors consider Greens

functions like

$$\langle 0|\bar{d}(z)\gamma_5 u(z)Q_{\pm}(x)\bar{u}(y)\gamma_5 s(y)\,|0\rangle \tag{20}$$

on the lattice. Wick contractions lead to the so-called "eight-graph" (Fig. 9a) and "eye--graph" (Fig. 9b). It should be noted that the u-quark (c-quark) loop in Fig. 9b is not a pure QCD-loop because of the weak interaction at point x, and this loop should therefore *not* be removed in the so-called quenched approximation used in lattice QCD. Basically Fig. 9a corresponds to amplitudes obtained from the left-left interactions considered in Ref. [1] (see the diagrams in Fig. 1 and 3) while the "eye-graph" corresponds basically to the penguin diagram (see Fig. 6). The calculations use an ultraviolet cut-off $\pi/a \simeq 3$ GeV, where a is the lattice spacing. For further details see Ref. [9]. It is found that the "eye--graphs" dominate significantly, and the ratio in Eq. (4) is found to be ~ 20. However, these calculations are still in an early stage.

b) QCD sum rules

Recently, Guberina, Pich and de Rafael have calculated $K \to \pi\pi$ amplitudes using QCD sum rules [10, 12, 27]. These authors consider the effective Hamiltonian in Eq. (8) and its counterpart within chiral Lagrangian theory [4, 5]

$$\mathscr{L}(\Delta S = 1) = g(\Delta I = 1/2)\mathscr{L}^{(1/2)} + g(\Delta I = 3/2)\mathscr{L}^{(3/2)}, \tag{21a}$$

where $\mathscr{L}^{(1/2)}$ and $\mathscr{L}^{(3/2)}$ represent the $\Delta I = 1/2$, and the $\Delta I = 3/2$ part of the interaction, respectively. The $\mathscr{L}^{(\,)}$'s in (21a) are written in terms of the chiral fields, for instance

$$\mathscr{L}^{(1/2)} \sim \mathrm{Tr}\,\{\lambda^6 \partial_\mu U^\dagger \partial^\mu U\}; \qquad U = \exp\left\{i\frac{\lambda^a \pi^a}{f}\right\}, \tag{21b}$$

where λ^a and π^a; $a = 1, \ldots, 8$; are the SU(3) flavour matrices and octet mesons, respectively ($f_K = f_\pi = f$ in the SU(3) limit). The authors study the two point functions

$$\langle 0|\mathrm{T}\{H_W^{(R)}(x)H_W^{(R)}(0)\}\,|0\rangle, \tag{22a}$$

$$\langle 0|\,\mathrm{T}\,\{\mathscr{L}^{(R)}(x)\mathscr{L}^{(R)}(0)\}\,|0\rangle, \tag{22b}$$

where R refers to a part of H_W or $\mathscr{L}(\Delta S = 1)$ corresponding to a given representation of SU(3) flavour. (22a) contains quark and gluon condensates, and the imaginary part of (22b) involves

$$\sum_\Gamma |\langle 0|\mathscr{L}^{(R)}|\Gamma\rangle|^2,$$

where the sum runs over mesonic intermediate states $\Gamma = K\pi$, $K\pi\pi$, $--$. By means of finite energy sum rules one may make contact between the functions in (22), and the couplings $g(\Delta I = 1/2)$ and $g(\Delta I = 3/2)$ in (21a) can be determined. While the obtained value for $g(\Delta I = 3/2)$ is in good agreement with experiment [12], the obtained value for $g(\Delta I = 1/2)$ is an order of magnitude too small [10]. That is, the method fails to explain the $\Delta I = 1/2$ rule. One may possibly find this surprising because the applied method is rather

close to a "first principle calculation". The same method gave the value 0.33 for the B-parameter in $K^0-\bar{K}^0$ mixing [27]. A slightly different method is used for $K^0-\bar{K}^0$ mixing by Decker [28], who considers a three point function involving $H_W^{(R)}$ and two axial currents with the flavour content of the two involved mesons. The obtained value for the B-parameter is $\simeq 0.55$.

c) Instanton effects

Konishi and Ranfone [29] have pointed out that instanton effects induce new $\Delta S = 1$ operators (see Fig. 10) not included by the authors of Refs [1] and [2]. As a typical example, consider

$$H_W^{\text{Inst.}} = \hat{G} C_{\text{Inst.}} Q_{\text{Inst.}}, \tag{23a}$$

$$Q_{\text{Inst.}} = \tfrac{1}{2}\{\bar{u}_R s_L \bar{d}_R u_L - \tfrac{1}{4}\bar{u}_R \sigma_{\mu\nu} s_L \bar{d}_R \sigma^{\mu\nu} u_L + \ldots\}. \tag{23b}$$

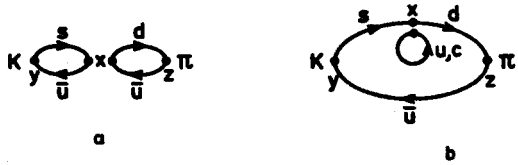

Fig. 9. Diagrams considered in the lattice approach of Ref. [9] a) The "eight-graph". b) The "eye-graph"

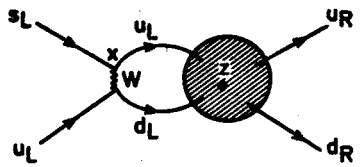

Fig. 10. Diagram for the instanton induced operator $H_W^{\text{Inst.}}$. The shaded region represents the instanton, which may flip the quark helicities

Note that this is (like the penguin operators) an operator of left-right type. In a modified RGE treatment it is found that $|C_{\text{Inst.}}| \gtrsim |C_{\text{LR}}|$. That is, (23) is at least as important as the penguin left-right part of the effective Hamiltonian in Eq. (16). ($C_{\text{Inst.}}$ includes the effect instanton size $\varrho < 1/\mu$, while contributions due to $\varrho > 1/\mu$ is regarded to be part of the matrix element). As we have seen in Section 2b, this is probably not enough to explain the $\Delta I = 1/2$ rule — but to draw a conclusion one has to wait for a further study of this mechanism (including $\varrho > 1/\mu$ effects). Anyway, instanton effects might at least provide a part of the observed $\Delta I = 1/2$ enhancement.

d) $1/N$ expansion

An analysis of $K \to \pi\pi$ decays by means of the $1/N$ expansion has recently been performed by Buras and Gerard [30]. The analysis can be visualized by quark diagrams related to the vacuum insertion approximation. The method makes use of relations like

$$\langle 0|\bar{u}_i \gamma^\mu L s_j|K\rangle = \frac{1}{N_c}\delta_{ij}\langle 0|\bar{u}\gamma^\mu L s|K\rangle \tag{24}$$

and the colour matrix relation (10). Keeping only the leading order in $1/N$, it is found that the theoretical value of the ratio r in Eq. (4) is improved. (An improvement of theoretical estimates of charmed decay processes is also obtained [31]). Depending on the values of C_{LR} a theoretical value for r of order 20 is obtained. In the real world we know that the number of colours is 3, which is not a very big number, and the $1/N$ expansion method applied to non-leptonic decays has recently been questioned by other authors [32]. However, in a very recent paper [33], the authors of Refs [30, 31] maintain their original conclusion.

e) Other approaches to $K \to \pi\pi$

Some other approaches to $K \to \pi\pi$ decays, which I will not talk about in detail, also exist in the literature. Pham and Sutherland [34] argue that intermediate D-meson states in the $K \to \pi$ transition may explain the $\Delta I = 1/2$ rule. Galić has given a "microscopic framework" involving non-local meson-quark vertices [35]. Approaches in terms of Regge poles and dispersion relations have also been given [36, 37].

4. Low momentum penguin contributions

a) A new philosophy

In this Section I will still consider the penguin diagram as the possible explanation of the $\Delta I = 1/2$ rule. But it will be assumed that the penguin diagram is not short distance dominated. In other words, $\ln(m_c^2/\mu^2)$ is not a leading log, C_{LR} is too small at the scale $\mu \sim 1$ GeV, and the quarks in the penguin loop feels confinement for loop momenta below some scale $\Lambda \lesssim m_c$. We make the following idealization: The loop momentum region is divided in a "high momentum" (HMR) and a "low momentum" (LMR) region at a scale $\Lambda \sim 1$ GeV $\lesssim m_c$. In the HMR ordinary perturbative QCD is valid, while in the LMR confinement effects have to be taken into account in some way. For the c-quark loop, m_c acts essentially as an effective infrared cut-off (just as the W-mass acts as an ultraviolet cut-off). Thus the c-quark loop belongs entirely to the HMR, while the u-quark loop gets contributions from both regions. In the HMR, the u- and c-quark loops approximately cancel, vizualized in the leading log approximation:

$$C_{LR} \sim \ln(M_W^2/\Lambda^2) - \ln(M_W^2/m_c^2) = \ln(m_c^2/\Lambda^2). \tag{25}$$

As pointed out previously, this is a dubious expression, but we assume that C_{LR} is small at $\mu = \Lambda$. Thus we are mainly left with u-quark contributions for loop momenta below Λ. In this region (LMR) we have to use a model which can take into account such low loop momenta. In some recent papers [6–8] applications of the philosophy described above are performed in terms of the MIT-bag model [38] and a chiral model with a mixed quark--meson phase [39]. This will be described in the next subsections.

b) The "bagged penguin"

The philosophy described in the preceding subsection was used in Ref. [6] by applying the MIT-bag model in the LMR. This was done by replacing the free quark propagators

by confined propagators written in terms of MIT-bag wave functions:

$$S(x, y) = -i \sum_N \{\theta(x_0 - y_0)\psi_N(x)\overline{\psi_N(y)} - \theta(y_0 - x_0)\psi_N^C(x)\overline{\psi_N^C(y)}\}, \tag{26}$$

where the sum runs over different modes N, and the superscript C means charge conjugation for the anti-quark modes. The amplitude for the penguin diagram (Fig. 6) may then be written

$$A_P \sim \alpha_S \hat{G}[C_+ + C_-] \iint_{\text{Bag}} d^4x d^4y J_\mu^a(x; \text{s} \to \text{d}) \Pi^{\sigma\mu}(x, y) A_\sigma^a(y; \bar{q}), \tag{27}$$

where $\Pi^{\sigma\mu}$ is a vacuum polarization like tensor:

$$\Pi^{\sigma\mu}(x, y) = \text{Tr}\{S(x, y)\gamma^\sigma S(y, x)\gamma^\mu L\}, \tag{28}$$

$J_\mu^a(\text{s} \to \text{d})$ is a left-handed coloured current for the s → d transition, and $A_\sigma^a(\bar{q})$ is the colour electric potential which can be deduced from the coloured quark current [38, 40]. $S(x, y)$ is a sum over quark modes. Thus $\Pi^{\sigma\mu}(x, y)$ is a double sum over bag model quark modes for the left and right part of the quark loop in Fig. 6. To obtain the contribution from the LMR, this double sum should run over modes corresponding to energy-momenta below Λ. For $\Lambda \simeq m_c$, one has to include (N, N') and (N', N) = (1S, 1P), (1S, 2P) and (2S, 1P) with $j = 1/2$ and 3/2 for the P-states (Note that one needs one S- and one P-quark to get a contribution. Thus the quark-antiquark pair in the loop has positive parity.) It is found that the low momentum contributions calculated from (27) are in fact more important than the standard short distance contribution given by C_{LR}. Even if (27) represents a long distance effect, the result can be parametrized in terms of an effective penguin coefficient for the K → π transition

$$C_{LR} \to C_P(\text{Bag}) \simeq (3 \text{ to } 5) \times C_{LR}. \tag{29}$$

It should be noted that according to our philosophy, low momentum contributions to the loop diagram in Fig. 3 should also be calculated. Such effects may be parametrized as modifications of the coefficients $C_\pm$ of Ref. [1] (probably of order 10%). While these (and more general the C_i's of Eq. (8)) are process independent, the low momentum loop contributions are in general process dependent. For instance, C_P(Bag) is smaller for the weak baryonic transition $\Omega \to \Xi^*$ to be used in the process $\Omega \to \gamma\Xi$, mainly due to bigger bag radii for the baryons. Thus an increase of the (low momentum) penguin effect in the case of K → ππ does not violate the upper limit of the process $\Omega \to \gamma\Xi$ [18].

The result in (29) is of course welcome. However, in bag model calculations one cannot control the chiral constraint in Eq. (3c) because the bag model is static (i.e. the three momenta of the mesons are zero). Moreover, the bag model has trouble with chiral invariance, and one may wonder if the amplitude obtained from (27) should — as in the case of Eq. (17) — be modified [14] and suppressed by some mass factor. To answer this question, one needs a model with chiral invariance, and which can account for the mo-

mentum dependence of the amplitude (see Eq. (3c)). Moreover, the model should include quarks in order to have a penguin diagram. Calculations within such a model [39] will be considered in the next subsection.

c) The "chiral penguin"

Georgi and Manohar [39] have introduced an effective chiral field theory which fits nicely into the philosophy of subsection a). This model has three phases. The chiral symmetry breaking scale Λ_χ is assumed to be separated from the confinement scale Λ_{QCD}. More explicitly, one uses $\Lambda_\chi \simeq 1$ GeV. Above the scale Λ_χ (i.e. in the HMR) we have the standard perturbative QCD phase with gluons and current quarks. For loop momenta below Λ_χ down to $\sim \Lambda_{QCD}$ there is a mixed phase with gluons, constituent quarks and Goldstone octet mesons (π, K, η). Below the scale $\sim \Lambda_{QCD}$ gluons and quarks are integrated out, and we are left with chiral interactions among mesons of the well known form

$$\mathscr{L} \sim \mathrm{Tr}\,\{\partial_\mu U^\dagger \partial^\mu U\} \tag{30}$$

with U given by Eq. (21b). In the mixed phase, there are QCD interactions and chiral interactions of the form (30). In addition there are meson quark interactions $\sim (g_A/f) p \cdot \gamma\gamma_5$, where p is the meson momentum. In the mixed phase, the total axial vector current is

$$j^a_{A,\mu} = g_A \bar{\psi} \gamma_\mu \gamma_5 \tfrac{1}{2} \lambda^a \psi - f \partial_\mu \pi^a, \tag{31}$$

where ψ is the SU(3) flavour triplet field and g_A is the axial vector coupling at quark level. The first term in (31) gives rise to a quark loop contribution to f_π; at one loop level as a quark--antiquark loop for $\pi^- \to d\bar{u} \to W^-$. Such a loop diagram needs a counterterm to keep the physical f_π at $p^2 = m_\pi^2$. The mixed phase effective theory is non-renormalizable, but Λ_χ is regarded as a physical ultraviolet cut-off for the theory (loop diagrams will typically generate new higher dimensional operators suppressed by powers of Λ_χ^{-1}). The model contains a direct $K \to \pi$ transition from Eq. (21) (this term corresponds to the vacuum insertion approximation, Eq. (13) with $Z_\pm = 1$), and $K \to \pi$ transitions through quark loops.

Using the quark meson coupling described above, the low loop momentum penguin diagram corresponding to a $K \to \pi$ transition is represented by the "chiral penguin" diagram in Fig. 11. The effective Hamiltonian of Ref. [1] renormalized at $\mu = \Lambda_\chi$ is acting

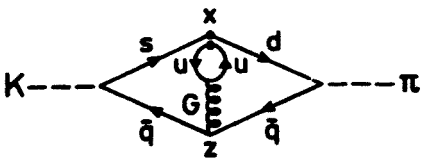

Fig. 11. The "chiral penguin" diagram

at point x (at the upper vertex of the diagram). For simplicity, we neglect penguin left--right operators (i.e. $C_{LR} \simeq 0$) at $\mu = \Lambda_\chi$. The "chiral penguin" diagram in Fig. 11 may look nasty, but handled with care, it is possible to extract the dominating parts. In the

following some details from the calculation will be given: The $s \to dG$ loop is proportional to a coloured current for $s \to d$

$$[\bar{d}\gamma_\mu L t^a s] \cdot F_P(k^2) k^2 [g^{\mu\nu} - k^\mu k^\nu / k^2], \tag{32}$$

k being the gluon (G) momentum. The factor k^2 is cancelled by the gluon propagator $(k^2)^{-1}$ (because of the tensor $[g^{\mu\nu} - k^\mu k^\nu / k^2]$ in (32), the gauge dependent part of the gluon propagator drops out, and the result is gauge invariant with respect to QCD). The loop factor $F_P(k^2)$ has the dominant behavior $\sim \ln(\Lambda_\chi^2)$. Using (32) we are essentially left with a two loop calculation over a quark momentum (p) and the gluon momentum (k). The term $\sim g^{\mu\nu}$ in (32) gives the local four-quark penguin operators within the standard approach [2, 3]. The term $\sim k^\mu k^\nu$ gives non-local penguin operators which cannot be neglected when the quarks are far off-shell, which is the case when the one loop result (32) is inserted in a higher loop diagram [7, 8, 41]. For the "local part" $\sim g^{\mu\nu}$ one may use a Fierz transformation to obtain an expression which is essentially the product of two one-loop expressions. For the non-local contribution, which turn out to be $-1/4$ of the "local", the calculation is, however, more cumbersome. The gluon vector current at the lower vertex (point z in Fig. 11) can be divided into a left (L) and a right (R)-handed part, while the upper vertex (point x) is pure left handed. Thus the amplitude due to the "chiral penguin" diagram can, as described below (16), be divided into LL and LR parts. It is then found that the LR "local" part is suppressed by at least Λ_χ^{-4} compared to the LL "local" part, and is numerically unimportant. Doing the integral over the quark momentum (p) first, the result is $\sim \ln(\Lambda_\chi^2)$ and then the integration $\int d^4k$ over gluon momentum (k) gives a factor $\sim \Lambda_\chi^4$. Further details are given in Ref. [8].

Collecting factors, the formally dominating behaviour of the "chiral penguin" diagram is [7, 8]

$$\sim [(g_A/f)^2 p_K \cdot p_\pi] \left[\frac{\alpha_S}{\pi} \ln(\Lambda_\chi^2)\right] \cdot \left[\frac{\Lambda_\chi^4 \ln(\Lambda_\chi^2)}{(4\pi)^4}\right] \tag{33a}$$

$$\simeq \frac{\alpha_S}{\pi} [\ln(\Lambda_\chi^2)]^2 f^2 p_K \cdot p_\pi. \tag{33b}$$

In (33a), the first factor is due to the product of $K^- s\bar{u}$ and $\pi^- d\bar{u}$ vertices. The two other factors are due to the loop integration as described above. Going from (33a) to (33b), the relation

$$\Lambda_\chi \simeq 4\pi f_\pi \tag{34}$$

is used. It is shown in Ref. [39] that this relation has to be valid in order to get meaningful loop calculations in the mixed phase. The result (33) is formally highly divergent if the cut-off Λ_χ increases. One reason for this is that the result (32) for the $s \to dG$ one loop is proportional to k^2 which is later to be integrated over. Also in other contexts the penguin diagram may give bigger results than naively expected when inserted in higher loops [41].

It should be noted that (33) satisfies the chiral constraint in Eq (3c). The result of the "chiral penguin" can be written in terms of an amplitude D as in Eq. (3):

$$D_{\chi P}(\Delta I = 1/2) = \frac{\alpha_S}{\pi} g_A^2[C_+ + C_-]F, \tag{35}$$

where $C_\pm$ are the coefficients in (9a) and (12) for $\mu = \Lambda_\chi$, and the factor $F \simeq 8$ contains the result of the loop calculation. A good analytical approximation for F is

$$F \simeq \left[\ln\left(\frac{\Lambda_\chi^2}{m^2}\right) - 1\right]\left[\ln\left(\frac{\Lambda_\chi^2}{m^2}\right) + \frac{9}{2}\right], \tag{36}$$

where m is the constituent quark mass (that is, $\Lambda_\chi/m \simeq 3$). We observe that the formally non-leading terms in (34), which are obtained from a detailed analysis [8] of the loop diagram in Fig. 11, are numerically important. From (35) and (13) we obtain the following ratio between $\Delta I = 1/2$ and $\Delta I = 3/2$ amplitudes

$$r = \frac{D(\Delta I = 1/2)_{\text{Tot}}}{D^{(\text{LL})}(\Delta I = 3/2)} = \tfrac{1}{2}\left[1 + \frac{3C_-Z_-}{2C_+Z_+}\right] + \frac{\alpha_S}{\pi}\frac{8g_A^2}{9Z_+}\left[1 + \frac{C_-}{C_+}\right]F, \tag{37}$$

which includes the old result (14) due to the effective Hamiltonian in Eq. (9).

Now, a problem is that we do not know the numerical values for α_S and g_A below Λ_χ. It should be emphasized that α_S in the Eqs (33, 35, 37) is not the α_S of ordinary QCD. The quark-gluon coupling in the mixed phase will in fact also (in addition to quark-gluon interactions) be renormalized by meson-quark interactions, as indicated in Fig. 12. It seems

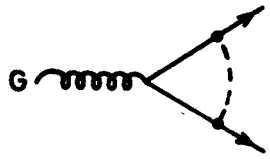

Fig. 12. Loop correction to the quark-gluon coupling in the mixed phase. The dashed line represents octet mesons

that the perturbative quark gluon coupling in the mixed phase will decrease with decreasing loop momentum-opposite to ordinary QCD. It is fundamentally nothing wrong with this because strong interactions due to soft gluons are thought to be mimicked by the chiral interactions in (30). In Ref. [39], $\alpha_S \simeq 0.3$ and $g_A \simeq 0.75$ are used to fit the observed baryon mass splittings and the axial vector coupling at baryon level, respectively. We will however argue that these are the values to be used at very low momenta ($\sim \Lambda_{\text{QCD}}$ and/or $\sim m_\pi$), while the values to be used just below Λ_χ are higher. The momentum dependence of α_S and g_A for momenta between $\sim \Lambda_{\text{QCD}}$ and Λ_χ should in principle be calculable in a coupled RGE calculation. However, this is a somewhat cumbersome task to be postponed to future work. In our case the loop integrals are dominated by momenta just below Λ_χ, and it seems to be reasonable to use effective values $\alpha_S \simeq 0.5$ to 0.7 and $g_A \simeq 0.9$ for our mixed phase

calculations. Using in addition $Z_+ \simeq 0.6$ to 0.8, we will typically obtain

$$r \sim 10 \text{ to } 20 \tag{38}$$

which is roughly half the needed enhancement. To obtain the experimental value $r \simeq 32$, one has to put $\alpha_S \simeq g_A \simeq 1$ and $Z_+ \simeq 0.5$, which is probably unrealistic. But still the result is encouraging and points towards a better understanding of the $\Delta I = 1/2$ rule.

5. *Conclusion and discussion*

I have given a short presentation of the standard short distance approach [1–3] to non-leptonic decays and tried to explain why it does not provide a satisfactory explanation of the $\Delta I = 1/2$ rule in $K \to \pi\pi$ decays. Further, I have described and advocated some long distance approaches to the $\Delta I = 1/2$ problem. Especially, I have considered the low loop momentum penguin approach [6–8] which seems to give promising results. I will give some comments on this approach below:

(*i*) In the "chiral penguin" approach the enhancement of the $\Delta I = 1/2$ amplitude is obtained in terms of the chiral symmetry breaking scale Λ_χ, which I find nice and interesting.

(*ii*) The low momentum penguin approach (both "bagged" and "chiral") make no use of the left-right (LR) penguin *operators* of SVZ [2]. This is done for simplicity and because their coefficients are probably small. However, as pointed out in previous papers [18, 23], C_{LR} is not zero even at $\mu = m_c$. That is, the GIM-cancellation is only effective in the leading log approximation (16c). In a very recent paper [33] it is announced that a careful treatment shows that C_{LR} is roughly twice as big as given in previous papers [2, 3]. This is due to incomplete GIM-cancellation for loop momenta above $\mu = m_c$. This effect could increase the effect of the penguin diagram somewhat more than found in (37).

(*iii*) The original idea [2] was that the new LR operators induced by the penguin diagram was responsible for the $\Delta I = 1/2$ rule. Later it was found that the amplitude due to penguin operators were suppressed compared to the original expression (17), due to chiral symmetry [4, 14]. As pointed out above (see Section 4c), left-right contributions from the "chiral penguin" diagram are also suppressed (and negligible). The amplitude in (37) is completely due to the left-left part of the "chiral penguin" diagram. As was done in the "bagged penguin" approach, the result (37) could be parametrized in terms of an "effective chiral penguin coefficient" to be compared to C_{LR}. But this is rather unnatural when the "chiral penguin" LR amplitude turns out to be unimportant.

(*iv*) It should be emphasized that even if the result (37) is encouraging, all effects to a given order in α_S and g_A have not been considered. However, as pointed out in the previous Section, when the penguin (one-) loop diagram is embedded in a higher loop diagram, one often gets an enhancement. Therefore other effects to the same order are not expected to be as important as the result (37). Such effects are for instance loop effects to correct for the vacuum insertion approximation, which in this paper is taken care of by means of the phenomenological constants $Z_\pm$.

(*v*) Instead of relying on soft-pion limits and pion reduction, one should rather consider

the $K \to \pi\pi$ amplitude directly, which is possible within the model of Ref. [39]. Before having calculated all loop effects to a given order, one cannot draw a final conclusion concerning $K \to \pi\pi$ amplitudes within the mixed phase model [39]. However, there are at least two problems to face in performing such a program. First, recent loop calculations [42] within ordinary chiral theory give large corrections. This may signalize a breakdown of chiral perturbative theory. But the situation could be different with the theory including a cut-off and a mixed phase (which implies additional diagrams including quark loops). Second, performing a systematic analysis of the weak Hamiltonian in the different phases, one may have trouble with the matching conditions of the weak operators at the phase transition scales Λ_{QCD} and Λ_χ.

(*vi*) It has often been claimed that if the penguin diagram is responsible for the $\Delta I = 1/2$ rule, then the theoretical value obtained within the standard model for the CP-violating quantity ε'/ε might be too big compared to the experimental value. However, sticking to the philosophy of Section 4, the explanation of ε' and the $\Delta I = 1/2$ rule are now decoupled because the CP-violating penguin contribution $\sim \ln (m_t^2/m_c^2)$ still belongs to the perturbative QCD regime.

(*vii*) Lattice calculations seem to indicate that confinement and chiral symmetry breaking takes place at roughly the same temperature, which should indicate that Λ_{QCD} and Λ_χ are of the same order of magnitude. To assume a chiral symmetry breaking scale $\Lambda_\chi \simeq 1$ GeV may therefore seem radical. However, a recent analysis of $K \to 2\pi$ and $K \to 3\pi$ decays indicates that there is an intrinsic scale ~ 1 GeV in the data of these processes [44]. Anyway, the model of Ref. [39] may therefore still have phenomenological interest.

(*viii*) I have not considered to what extent the long distance approaches presented above are equivalent or not. But some of them are obviously based on similar ideas. For instance the lattice approach [9], where the u (or c)-quark loop is bathing in a gluon field, and the low momentum penguin approach [6–8] seem to be qualitatively close. Moreover, the inclusion of additional mesonic low momentum effects in the penguin coefficient C_{LR} made in Ref. [33] seems to be based on similar ideas — whether one sticks to the $1/N$-expansion method [30, 31] or not.

To conclude, even if it is too early to claim that the $\Delta I = 1/2$ rule is now understood theoretically, some recent calculations show encouraging results. These indicate that a better understanding of the $\Delta I = 1/2$ rule might be obtained in terms of long distance effects. Especially, the penguin diagram seems to be enhanced by low loop momenta. Thus the original proposal [2] that the penguin diagram is responsible for the $\Delta I = 1/2$ rule still seems to be relevant-but now in the long distance regime. Anyway, more work has still to be done on this longstanding problem.

It is a pleasure to thank the organisers for warm hospitality.

REFERENCES

[1] a) M. K. Gaillard, B. W. Lee, *Phys. Rev. Lett.* **33**, 108 (1974); b) G. Altarelli, L. Maiani, *Phys. Lett.* **52B**, 35 (1974).

[2] a) A. I. Vainshtein, V. I. Zakharov, M. A. Shifman, *Pis'ma Zh. Eksp. Teor. Fiz.* **22**, 123 (1975)

(*Sov. Phys. JETP Lett.* **22**, 55 (1975)); b) A. I. Vainshtein, V. I. Zakharov, M. A. Shifman, *Zh. Eksp. Teor. Fiz.* **72**, 1275 (1977) (*Sov. Phys. JETP* **45**, 670 (1977)); c) M. A. Shifman, A. I. Vainshtein, V. I. Zakharov, *Nucl. Phys.* **B120**, 316 (1977).

[3] J. F. Donoghue, E. Golowich, W. A. Ponce, B. R. Holstein, *Phys. Rev.* **D21**, 186 (1980).

[4] Y. Dupont, T. N. Pham, *Phys. Rev.* **D29**, 1368 (1984); T. N. Pham, *Phys. Lett.* **145B**, 113 (1984).

[5] J. A. Cronin, *Phys. Rev.* **161**, 1499 (1967).

[6] J. O. Eeg, *Phys. Lett.* **155B**, 115 (1985).

[7] J. O. Eeg, *Phys. Lett.* **171B**, 103 (1986).

[8] J. O. Eeg, *Z. Phys.* **C33**, 227 (1986).

[9] C. Bernard, T. Draper, G. Hockney, A. M. Rushton, A. Soni, *Phys. Rev. Lett.* **55**, 2770 (1985).

[10] A. Pich, B. Guberina, E. de Rafael, *Nucl. Phys.* **B277**, 197 (1986).

[11] R. Decker, *Z. Phys.* **C29**, 31 (1985).

[12] B. Guberina, A. Pich, E. de Rafael, *Phys. Lett.* **163B**, 198 (1985).

[13] S. L. Glashow, J. Iliopoulos, L. Maiani, *Phys. Rev.* **D2**, 1285 (1970).

[14] a) J. F. Donoghue, *Phys. Rev.* **D30**, 1499 (1984); b) M. B. Gavela, A. Le Yaonanc, L. Oliver, O. Pene, J. C. Raynal, *Phys. Lett.* **148B**, 253 (1984).

[15] N. Bilić, B. Guberina, *Phys. Lett.* **150B**, 311 (1985); *Z. Phys.* **C27**, 399 (1985).

[16] M. A. Ahmed, *Phys. Rev.* **D32**, 671 (1985).

[17] M. Milošević, D. Tadić, J. Trampetić, *Nucl. Phys.* **B187**, 514 (1981).

[18] J. O. Eeg, *Z. Phys.* **C21**, 253 (1984).

[19] J. F. Donoghue, E. Golowich, B. R. Holstein, *Phys. Rev.* **D12**, 1386 (1976); **D15**, 1341 (1977); **D23**, 1213 (1981); J. F. Donoghue, E. Golowich, *Phys. Lett.* **69B**, 437 (1977); H. Galić, D. Tadić, J. Trampetić, *Nucl. Phys.* **B158**, 306 (1979); *Phys. Lett.* **89B**, 249 (1980).

[20] D. Tadić, J. Trampetić, *Nucl. Phys.* **B171**, 471 (1980); M. B. Gavela, A. Le Yaouanc, L. Oliver, O. Pene, J. C. Raynal, T. N. Pham, *Phys. Lett.* **101B**, 417 (1980); K. G. Rauh, *Z. Phys.* **C10**, 81 (1981); P. Colić, J. Trampetić, D. Tadić, *Phys. Rev.* **D9**, 2286 (1982).

[21] M. Praszałowicz, J. Trampetić, *Phys. Lett.* **161B**, 169 (1985); J. F. Donoghue, E. Golowich, Y.-C. R. Lin, *Phys. Rev.* **D32**, 1733 (1985).

[22] A. J. Buras, W. Słomiński, *Nucl. Phys.* **B253**, 231 (1985).

[23] H. Galic, SLAC-Pub-2602, 1980, unpublished; J. Finjord, *Nucl. Phys.* **B181**, 74 (1981).

[24] N. Cabibbo, G. Martinelli, R. Petronzio, *Nucl. Phys.* **B244**, 381 (1984); R. C. Brower, G. Marturana, M. B. Gavela, R. Gupta, *Phys. Rev. Lett.* **53**, 1318 (1984).

[25] C. Bernard, T. Draper, A. Soni, H. D. Politzer, M. B. Wise, *Phys. Rev.* **D32**, 2343 (1985); A. Le Yaouanc, L. Oliver, O. Pene, J. C. Raynal, LPTHE 86/27.

[26] R. J. Crewther, *Nucl. Phys.* **B264**, 277 (1986).

[27] A. Pich, E. de Rafael, *Phys. Lett.* **158B**, 477 (1985).

[28] R. Decker, *Nucl. Phys.* **B277**, 661 (1986).

[29] K. Konishi, S. Ranfone, *Phys. Lett.* **172B**, 417 (1986).

[30] A. J. Buras, J.-M. Gerard, *Nucl. Phys.* **B264**, 371 (1986).

[31] A. J. Buras, J.-M. Gerard, R. Rückl, *Nucl. Phys.* **B268**, 16 (1986).

[32] R. S. Chivukula, J. M. Flynn, H. Georgi, *Phys. Lett.* **171B**, 453 (1986).

[33] W. A. Bardeen, A. J. Buras, J.-M. Gerard, *Phys. Lett.* **180B**, 133 (1986).

[34] T. N. Pham, D. G. Sutherland, *Phys. Lett.* **135B**, 209 (1984); T. N. Pham, Talk at the XXIth Rencontre de Moriond, March 1986, to appear in the proceedings.

[35] H. Galic, *Phys. Rev.* **D31**, 2363 (1985); *Z. Phys.* **C29**, 519 (1985).

[36] G. Nardulli, G. Preparata, D. Rotondi, *Phys. Rev.* **D27**, 557 (1983).

[37] N. F. Nashrallah, N. A. Papadopoulos, K. Schilcher, *Phys. Lett.* **134B**, 355 (1984).

[38] A. Chodos, R. L. Jaffe, K. Johnson, C. B. Thorn, *Phys. Rev.* **D10**, 2599 (1974); T. De Grand, R. L. Jaffe, K. Johnson, J. Kiskis, *Phys. Rev.* **D12**, 2060 (1975).

[39] A. Manohar, H. Georgi, *Nucl. Phys.* **B234**, 189 (1984); H. Georgi, *Weak interactions and modern particle theory*, Benjamin/Cummings Publ. Co. 1984.

[40] T. A. De Grand, *Ann. Phys.* **101**, 496 (1976).
[41] J. O. Eeg, I. Picek, *Phys. Lett.* **130B**, 308 (1983); *Nucl. Phys.* **B244**, 77 (1984); *Phys. Lett.* **B177**, 432 (1986).
[42] J. Bijnens, *Phys. Lett.* **152B**, 226 (1985); J. F. Donoghue, B. R. Holstein, *Phys. Lett.* **160B**, 173 (1985).
[43] A. G. Cohen, A. V. Manohar, HUTP-84/A025.
[44] J. F. Donoghue, E. Golowich, B. R. Holstein, *Phys. Rev.* **D30**, 2367 (1984).